

Published in final edited form as:

Am J Physiol Lung Cell Mol Physiol. 2006 November ; 291(5): L905–L911. doi:10.1152/ajplung.00543.2005.

3-Deazaadenosine mitigates arterial remodeling and hypertension in hyperhomocysteinemic mice

Alexander V Ovechkin, Neetu Tyagi, Utpal Sen, David Lominadze, Mesia M. Steed, Karni S. Moshal, and Suresh C. Tyagi

Department of Physiology and Biophysics, School of Medicine, University of Louisville, Louisville, Kentucky

Abstract

Chronic hyperhomocysteinemia (HHcy) is an important factor in development of arterial hypertension. HHcy is associated with activation of matrix metalloproteinases (MMPs); however, it is unclear whether HHcy-dependent extracellular matrix (ECM) accumulation plays a role in arterial hypertrophy and hypertension. We tested the hypothesis that in HHcy the mechanism of arterial hypertension involves arterial dysfunction in response to ECM accumulation between endothelial and arterial smooth muscle cells and subsequent endothelium-myocyte (E-M) uncoupling. To decrease plasma Hcy, dietary supplementation with 3-deazaadenosine (DZA), the *S*-adenosylhomocysteine hydrolase inhibitor, was administered to cystathionine β -synthase (CBS) knockout (KO) mice. Mice were grouped as follows: wild type (WT; control), WT+DZA, CBSKO, and CBSKO+DZA ($n = 4$ /group). Mean aortic blood pressure and heart rate were monitored in real time with a telemetric system before, during, and after DZA treatment (6 wk total). In vivo aorta function and morphology were analyzed by M-mode and Doppler echocardiography in anesthetized mice. Aorta MMP activity in unfixed cryostat sections was measured with DQ gelatin. Aorta MMP-2, MMP-9, and connexin 43 expression were measured by RT-PCR and Western blot analyses, respectively. HHcy caused increased aortic blood pressure and resistance, tachycardia, and increased wall thickness and ECM accumulation in aortic wall vs. control groups. There was a linear correlation between aortic wall thickness and plasma Hcy levels. MMP-2, MMP-9, and connexin 43 expression were increased in HHcy. In the CBSKO +DZA group, aortic blood pressure and levels of MMP and connexin 43 were close to those found in control groups. However, removal of DZA reversed the aortic lumen-to-wall thickness ratio in CBSKO mice, suggesting, in part, a role of vascular remodeling in the increase in blood pressure in HHcy. The results show that arterial hypertension in HHcy mice is, in part, associated with arterial remodeling and E-M uncoupling in response to MMP activation.

Keywords

cardiovascular dysfunction; aorta; echocardiography; extracellular matrix remodeling; in situ matrix metalloproteinase activity; cystathionine β -synthase; connexin; DQ gelatin; telemetry

Experimental and clinical studies have shown that chronic elevation of homocysteine (Hcy) levels, known as hyperhomocysteinemia (HHcy), is a significant independent risk factor for cardiovascular disease (31), particularly in the development of arterial hypertension and atherosclerosis (3, 24, 26). The mechanisms by which HHcy affects arterial wall and induces

arterial hypertension have remained unclear. It has been shown that HHcy leads to arterial damage (4) and increased arterial wall stiffness (2, 22).

Hcy is a product of methionine metabolism that under normal conditions is converted to cystathionine by cystathionine β -synthase (CBS). It has been established that mice carrying a disrupted CBS gene are adequate models for HHcy. Systemic vascular cells lacking CBS (7, 8) are the prime target for endothelial damage leading to arterial hypertension. It has been previously demonstrated that 3-deazaadenosine (DZA), a most potent inhibitor of *S*-adenosylhomocysteine hydrolase (SAHH) enzyme, prevents conversion of *S*-adenosylhomocysteine to Hcy and decreases formation of Hcy (13, 21). DZA binds to SAHH, resulting in the accumulation of *S*-adenosylhomocysteine and *S*-adenosylmethionine, and serves as a substrate for the enzyme, resulting in the significant accumulation of 3-deazaadenosyl-Hcy serving as an Hcy scavenger (1).

Studies in animal models demonstrated that HHcy could induce marked remodeling of the extracellular matrix (ECM) of the arterial wall by inducing elastinolysis through the activation of matrix metalloproteinases (MMPs) (10). Cardiovascular remodeling is associated with accumulation of ECM components between endothelial and muscle cells (16, 17) and is one of the most important factors of endothelial dysfunction (11, 14). Degradation of interstitial collagen and elastin by MMPs leads to increased ECM formation and endothelium-muscle uncoupling (17, 19), because the more collagen is degraded, the more of it is synthesized (28). There are more than 20 MMPs in the family, but increase in MMP-2 and -9 activities has a more pronounced effect during early and late phases of cardiovascular remodeling (27).

We hypothesized that HHcy induces arterial hypertension through the accumulation of ECM components between endothelial and arterial smooth muscle cells, which results in subsequent endothelium-myocyte (E-M) uncoupling in response to MMP activation.

MATERIALS AND METHODS

Wild-type (WT; B6.129PF2/J) and breeding pairs of CBS heterozygote ($-/+$) knockout (CBSKO; B6.129P2-*Cbs*^{tm1Unc}) mice aged 8–12 wk were obtained from Jackson Laboratories (Bar Harbor, ME). Mice were bred at the breeding facility of the University of Louisville School of Medicine. Homozygous mutants, completely lacking CBS, have 40- to 50-fold higher plasma Hcy levels and a very short life span. In this study, we used male heterozygous animals with plasma Hcy levels between 25 and 30 μ M, a well established model of HHcy (29). To normalize Hcy levels in CBSKO mice, during the experiments (32 days) dietary supplementation of DZA (Sigma, St. Louis, MO) was administered in the form of a specially prepared rodent laboratory chow with DZA (0.04 g/kg). To determine whether DZA induced changes in blood pressure and/or flow independent of the effects on ECM remodeling, the control group received a chow similar to that for the treatment group except for DZA. The animals were divided into four groups: WT, WT+DZA, CBSKO, and CBSKO treated with DZA (CBSKO+DZA). Four ($n = 4$) animals in each group were used. Although we did not measure SAHH activity, others have shown that DZA specifically and significantly reduces SAHH activity (13, 21). All experimental mice were exposed to a similar environment and procedures according to National Institutes of Health guidelines and approved by the Institutional Animal Care and Use Committee of the University of Louisville School of Medicine.

Echocardiography

Mice were anesthetized intraperitoneally with tribromoethanol (100 mg/kg). A Hewlett-Packard Sonos 7770 echocardiographic system equipped with a 15-MHz shallow-focus

21211A phased-array transducer was used for measurements of aortic function and morphology. The transducer probe was placed on the left hemi-thorax of mice in the partial left decubitus position. Two-dimensional targeted M-mode and pulsed-wave Doppler (PW) echocardiograms were obtained from a long-axis perspective to record aortic diameter/wall thickness and aortic blood time-averaged velocity (TAV) with ejection time, respectively. Aortic blood flow (ABF) was calculated as TAV (cm/s) \times aortic cross-sectional area (cm²) \times ejection time (s) \times HR (cycles/min) (18), where aortic cross-sectional area was calculated as $\pi \times (\text{aorta radius})^2$ and HR is heart rate. Only M-mode and PW echocardiograms with well-defined continuous interfaces of the aorta were collected.

Direct radiotelemetric measurements of aorta blood pressure and HR

Systolic/diastolic blood pressure and HR were measured continuously during experiment with a DSI (Data Sciences International; St. Paul, MN) telemetric system using a pressure transducer (PA-C20) surgically implanted into the aortic arch through the left common carotid artery as described previously (15, 30), starting after a 1-wk surgical recovery period. The data were analyzed with DSI Dataquest ART 3.1 software. At the end of each experiment, plasma samples and thoracic aortas were obtained from overanesthetized mice with arrested hearts. Body and heart weights were measured.

Plasma Hcy measurements

The level of Hcy in plasma was quantitatively analyzed with the Bio-Rad microplate enzyme immunoassay homocysteine assay (Bio-Rad Laboratories, Hercules, CA) and a SpectraMax M2 Analyzer (Molecular Devices, Sunnyvale, CA) according to the manufacturers' instructions. The data were expressed as Hcy concentration in plasma ($\mu\text{mol/l}$).

Masson trichrome staining

The frozen thoracic aortas were sectioned transversely at 10 μm with a cryostat (Leica Cryocut 1800, Leica Microsystems, Germany). To measure the deposition of collagen in the aortic wall, the sections were stained with a Masson trichrome kit (Richard Allan Scientific, Kalamazoo, MI). The images were taken with a "Q-color 3" digital camera on an IX81 inverted microscope with a $\times 100/1.35$ UPlanApo objective (Olympus).

In situ zymography with quenched fluorogenic gelatin

Aortas were cut from snap-frozen tissue blocks, and unfixed 10- μm sections were developed with an EnzChek gelatinase assay kit and a Prolong antifade kit (Molecular Probes, Eugene, OR) as described previously (9). MMP activity was detected on a Fluoview 1000 confocal laser microscope with a $10\times/0.30$ UPlanFI objective and an FITC filter (Olympus). Quantitative analysis was performed with Image Pro plus software (Media Cybernetics, Silver Spring, MD). Data were expressed as area (pixel²) of marker and averaged for each group.

MMP-2 and MMP-9 expression by RT-PCR

DNA-free total RNA was isolated from tissue with TRIzol reagent (GIBCO-BRL), and RNA (1 $\mu\text{g}/\mu\text{l}$) was used for preparation of first-strand cDNA with reverse transcriptase. The RNA samples were incubated (70°C, 5 min) with 1 μl of oligoprimers in a final volume of 5 μl . Samples were then incubated in 15 μl of a reaction buffer. Expression level of the RNA was determined from 2 μl of each cDNA sample. For amplification of the housekeeping gene, specific primers of glyceraldehyde-3-phosphate dehydrogenase (mouse GAPDH; GenBank accession number NM-008084) were used. Upstream (5'-TACATTTCCCCTTCTTACT-3') and downstream (3'-

CCACATTTGACGTCCAGAGA-5') primers for MMP-2 and MMP-9 were synthesized based on the mouse MMP-2 and MMP-9 mRNA sequences (GenBank). The denaturation step was set for 30 s at 94°C, annealing for 60 s at 60°C, and extension for 90-s cycles at 72°C. GAPDH samples were taken over 30 cycles, and MMP samples were taken over 35 cycles. PCR reactions were performed with a thermal cycler (Perkin-Elmer 9600) in 50 µl of 1× PCR buffer, 1.5 mM MgCl₂, each primer at 0.2 µM, 200 µM dNTP, and 1 U of *Taq* DNA polymerase (Invitrogen). Amplification mixtures were analyzed by 1% agarose gel electrophoresis.

Western blot analysis of connexin 43

Twenty-five micrograms of total protein from aortic homogenates was loaded in each well, run on 10% SDS-PAGE, and transferred to polyvinylidene difluoride membranes. The membranes were blotted with anti-connexin 43 monoclonal antibodies (Chemicon) as previously described (19). Secondary IgG-alkaline phosphatase was used for detection. Actin blots were used as a loading control. The bands were scanned and normalized with actin intensity. The gels were stained with Coomassie blue for protein.

Statistical analysis

The calculation of sample size ($n = 4$) provided a power of the test of 80%. Differences between groups were compared by one-way analysis of variance with repeated measurements and multiple comparisons (consideration given to within-sample variability of observations). Values are reported as means \pm SE. Correlation coefficient and linear regression analysis were used to determine the relationship between two variables. A probability level of $P < 0.05$ was used to indicate statistical significance.

RESULTS

Physiological parameters

Plasma Hcy levels were significantly increased in the CBSKO group compared with the control WT group and returned to control level in the CBSKO+DZA group. Similarly, mean arterial blood pressure (MAP) and HR in the CBSKO group (130 ± 1 mmHg and 520 ± 40 beats/min, respectively) were significantly higher than in WT controls (92 ± 1 mmHg and 435 ± 30 beats/min, respectively). These increases in MAP and HR were ameliorated in the CBSKO+DZA group (93 ± 1 mmHg and 469 ± 27 beats/min, respectively) (Table 1 and Fig. 1). We did not find any significant difference in MAP and HR data between WT and WT +DZA groups. Although body and heart weights were not significantly different in all groups, heart weight tended to increase in CBSKO mice ($P < 0.05$ compared with WT and CBSKO+DZA groups; Table 1), suggesting cardiac as well as vascular hypertrophy in HHcy mice.

Aortic remodeling

Echocardiographic data revealed significant increase in aorta wall thickness and significant decrease in aortic lumen/wall coefficient in the CBSKO group compared with WT and CBSKO+DZA mice (Table 1; Figs. 2 and 3A). In addition, increase in aortic wall focal fibrosis in the animals from the CBSKO group, compared with control, was mitigated in the CBSKO+DZA group (Fig. 4). The increase in vascular wall thickness is evident from the photographs in Fig. 4, where the increase in collagen (blue) and fibrosis is significantly higher in CBSKO than WT aortas. In addition, there appeared to be more elastic tissue in the WT aortas (Fig. 4B), suggesting greater elastic-vascular compliance in WT than CBSKO aorta. The elastic fibers in CBSKO mouse aortas were fragmented. This suggested remodeling in the aortas from CBSKO animals (Fig. 4C). Compared with WT animals, the

level of connexin 43 (cell uncoupling marker) expression was significantly increased in CBSKO animals, but when those animals were treated with DZA that increase was attenuated (Fig. 5).

ABF and resistance

Although aorta blood TAV was not significantly different between groups (Table 1 and Fig. 2), aortic resistance was significantly increased in CBSKO mice, but that increase was not detected in CBSKO+DZA animals (Fig. 3B).

MMP-2 and MMP-9 in aorta remodeling

Total MMP activity in aorta sections, estimated from the levels of gelatinolytic activity with DQ gelatin fluorescein-conjugated substrate, showed dramatic increase in gelatinolytic activity in CBSKO animals and a return to control levels in the CBSKO+DZA group (Fig. 6). Similarly, MMP-2 and MMP-9 mRNA expression in aorta tissue from the CBSKO group were significantly higher than in WT and CBSKO+DZA animals (Fig. 7). These data suggest that MMPs are involved in HHcy-induced aortic stiffness, hypertrophy, and remodeling.

Plasma Hcy levels, DZA, and aortic wall thickness

Plasma levels of Hcy were directly correlated ($r = 0.94$) with aortic wall thickness (Fig. 8A), suggesting the positive correlation of plasma Hcy levels and arterial hypertension. To provide an important clue as to whether the change in blood pressure was due to remodeling or hemodynamic changes, we performed experiments to determine the aortic lumen-to-wall thickness ratio as a measure of vascular remodeling and hypertrophy at *day 25* (at the time of DZA withdrawal when the systolic blood pressure is low) and again at *day 30* (when the pressure is back up) (Fig. 8B). The data suggest significant aortic wall thickness over these few days, supporting the premise that vascular remodeling is a key factor for systemic vascular resistance. In addition, the data suggest that the lowering of blood pressure in response to DZA was related to the regression of vascular remodeling and hypertrophy between 4 and 10 days after DZA was administered to the CBSKO mice. Aortic wall hypertrophic remodeling occurred between *days 25* and *30*, when the withdrawal of DZA led to increase in systolic blood pressure. These results suggest that vascular remodeling is one of the key factors in Hcy-mediated increase in blood pressure.

DISCUSSION

Remodeling by its very nature implies synthesis and degradation of ECM components in the vessel wall. MMP-2 and -9 specifically degrade elastin. Hcy induces MMP-2 and -9. The inhibitors of elevated Hcy decrease MMP activity and preserve the elastic contents of the vessel wall. The results of this study suggest that inhibition of Hcy production mitigates MMP activation and arterial remodeling in hyperhomocysteinemic mice.

A linear correlation between Hcy levels and systolic hypertension was demonstrated previously (24). A direct connection between aortic wall thickness and Hcy levels has also been shown (5, 25, 32). Our data also suggest that aortic wall thickness is positively associated with the levels of plasma Hcy and arterial hypertension. Although it is known that HHcy leads to arterial hypertension, to our knowledge aortic echography and direct radiotelemetric measurements of aortic blood pressure and HR in HHcy animals have not been reported previously. Our data showed that treatment with DZA is an effective tool in normalization of plasma Hcy, aortic blood pressure, and HR in the CBSKO HHcy model in mice (Table 1, Fig. 8).

Although the mechanisms of cardiovascular dysfunction in HHcy associated with arterial hypertension are still unknown (31), a strong implication of MMPs as potential mediators of cardiovascular remodeling is suggested (6). Others and we previously suggested (12, 19) a role of MMP activation and E-M uncoupling in cardiac remodeling and dysfunction in chronic heart failure. The results of this study showed that impaired arterial function in the HHcy model of arterial hypertension is also associated with MMP activation, ECM accumulation, and arterial remodeling.

Recently we demonstrated (20) that Hcy instigates a “negative vascular remodeling” or inward directed increase in arterial wall thickness and hypertension. The results of the present study are consistent with our previous report (23) that a relationship between Hcy level and thickness of the arterial wall may be a mechanism that is involved in causing arterial hypertension. Others reported that HHcy has only a marginal influence on aorta stiffness (22). In our study, echocardiographic and histological data suggested that aortic wall hypertrophy in mice with HHcy was associated with accumulation of ECM components. Although body weight was not significantly different between all groups, aorta wall thickness was positively correlated with the levels of plasma Hcy and arterial hypertension (Table 1, Fig. 8). We showed previously (19) that increased expression of connexin 43, the marker of cell uncoupling, was associated with ECM formation due to compensatory response to cell disintegration. The results of the present study showed that in animals from the CBSKO+DZA group, the significant increase in connexin 43 expression and ECM accumulation detected in CBSKO animals were ameliorated. We found that cardiovascular function in these animals was also impaired. The significant decrease in aortic lumen-to-wall ratio and significant increase in aortic resistance were correlated to the levels of plasma Hcy and arterial hypertension (Table 1 and Fig. 3).

Our hypothesis was that impaired arterial function in HHcy could be the consequence of ECM accumulation due to MMP activation. We found that the levels of MMP activation and ECM accumulation in CBSKO animals were significantly higher than in control animals. In animals with HHcy, collagenolytic activity and MMP-2 and MMP-9 gene expression in aorta tissue were dramatically increased and were correlated to aorta ECM deposition (Fig. 4), and the fact that these increases were mitigated by DZA treatment clearly indicated that MMPs play a crucial role in Hcy-mediated vascular remodeling.

In summary, the results of the present experiments demonstrate that in the HHcy model in mice impaired arterial function is associated with aorta wall hypertrophy due to ECM accumulation. Our study may suggest that increased Hcy levels lead to arterial hypertension through systemic artery remodeling, including vascular hypertrophy, as shown by the hemodynamic results detailed in Fig. 1. There is no decrease in aortic lumen-to-wall thickness ratio between *days 0* and *4*, yet there is a marked drop in systolic blood pressure over this time period (Fig. 1A); more dramatically, when DZA is withdrawn at *day 25* the systolic blood pressure increases within a few days. This may suggest that the drop in blood pressure at least acutely is due to a lowering of cardiac output (via a drop in pulse) or a drop in systemic vascular resistance. This may also suggest that the change in systolic blood pressure related to DZA use is probably a combination of hemodynamic changes and vascular remodeling. It is possible that Hcy may alter systolic blood pressure through both acute hemodynamic effects and vascular remodeling.

Acknowledgments

A part of this study was supported by National Heart, Lung, and Blood Institute Grants HL-71010 and HL-74185.

References

1. Aksamit R, Falk W, Cantoni G. Inhibition of chemotaxis by *S*-3-deazaadenosylhomocysteine in a mouse macrophage cell line. *J Biol Chem*. 1982; 257:621–625. [PubMed: 7054170]
2. Arcaro G, Fava C, Dagradi R, Faccini G, Gaino S, Degan M, Lechi C, Lechi A, Minuz P. Acute hyperhomocysteinemia induces a reduction in arterial distensibility and compliance. *J Hypertens*. 2004; 22:775–781. [PubMed: 15126920]
3. Boers G. Hyperhomocysteinemia as a risk factor for arterial and venous disease: a review of evidence and relevance. *Thromb Haemost*. 1997; 78:520–522. [PubMed: 9198207]
4. Boot M, Steegers-Theunissen R, Poelmann R, van Iperen L, Gittenberger-de Groot A. Homocysteine induces endothelial cell detachment and vessel wall thickening during chick embryonic development. *Circ Res*. 2004; 94:542–549. [PubMed: 14699014]
5. Bortolotto LA, Safar ME, Billaud E, Lacroix C, Asmar R, London GM, Blacher J. Plasma homocysteine, aortic stiffness, and renal function in hypertensive patients. *Hypertension*. 1999; 34:837–842. [PubMed: 10523370]
6. Ducharme A, Frantz S, Aikawa M, Rabkin E, Lindsey M, Rohde L, Schoen F, Kelly R, Werb Z, Libby P, Lee R. Targeted deletion of matrix metalloproteinase-9 attenuates left ventricular enlargement and collagen accumulation after experimental myocardial infarction. *J Clin Invest*. 2000; 106:55–62. [PubMed: 10880048]
7. Finkelstein JD. The metabolism of Hcy: pathways and regulation. *Eur J Pediatr*. 1998; 157:S40–S44. [PubMed: 9587024]
8. Finkelstein JD. Methionine metabolism in mammals. *J Nutr Biochem*. 1990; 1:228–237. [PubMed: 15539209]
9. Frederics W, Mook O. Metabolic mapping of proteinase activity with emphasis on in situ zymography of gelatinases: review and protocols. *J Histochem Cytochem*. 2004; 52:711–722. [PubMed: 15150280]
10. Giusti B, Marcucci R, Lapini I, Sestini I, Lenti M, Yacoub M, Pepe G. Role of hyperhomocysteinemia in aortic disease. *Cell Mol Biol (Noisy-le-grand)*. 2004; 50:945–952. [PubMed: 15704258]
11. Goette A, Juenemann G, Peters B, Klein HU, Roessner A, Huth C, Rocken C. Determinants and consequences of atrial fibrosis in patients undergoing open heart surgery. *Cardiovasc Res*. 2002; 54:390–396. [PubMed: 12062343]
12. Hu C, Chang HR, Hsu YH, Liu CJ, Chen HI. Ventricular hypertrophy and arterial hemodynamics following deprivation of nitric oxide in rats. *Life Sci*. 2005; 78:164–173. [PubMed: 16125730]
13. Jeong S, Ahn S, Lee J, Kim H, Kim J, Rhim H, Jeong S, Kim I. 3-Deazaadenosine, a *S*-adenosylhomocysteine hydrolase inhibitor, has dual effects on NF- κ B regulation. *J Biol Chem*. 1999; 274:18981–18988. [PubMed: 10383397]
14. Jessup M, Brozena S. Heart failure. *N Engl J Med*. 2003; 348:2007–2018. [PubMed: 12748317]
15. Kramer K, Kinter LB. Evaluation and applications of radiotelemetry in small laboratory animals. *Physiol Genomics*. 2003; 13:197–205. [PubMed: 12746464]
16. Mebazaa A, Wetzel R, Cherian M, Abraham M. Comparison between endothelial and great vessel endothelial cells: morphology, growth, and prostaglandin release. *Am J Physiol Heart Circ Physiol*. 1995; 268:H250–H259.
17. Moshal K, Tyagi N, Henderson B, Ovechkin A, Tyagi S. Protease-activated receptor and endothelial-myocyte uncoupling in chronic heart failure. *Am J Physiol Heart Circ Physiol*. 2005; 288:H2770–H2777. [PubMed: 15681708]
18. Niscimento R, Dehant P, Jimenez M, Dequeker J, Castela E, Choussat A. Calculation of the pulmonary to systemic flow ratio using echo-Doppler in septal defects—correlation with oximetry. *Rev Port Cardiol*. 1989; 8:35–40. [PubMed: 2631813]
19. Ovechkin A, Tyagi N, Rodriguez W, Hayden M, Moshal KS, Tyagi SC. Role of matrix metalloproteinase-9 in endothelial apoptosis in chronic heart failure. *J Appl Physiol*. 2005; 99:2398–2405. [PubMed: 16081621]
20. Reddy HK, Koshy SKG, Wasson S, Quan EE, Pagni S, Roberts AM, Joshua IG, Tyagi SC. Adaptive-outward and maladaptive-inward arterial remodeling measured by intracoronary

- ultrasound in hyperhomocysteinemia and diabetes. *J Cardiovasc Pharmacol Ther.* 2006; 11:65–76. [PubMed: 16703221]
21. Shea TB, Ashline D, Ortiz D, Milhalik S, Rogers E. The S-adenosyl homocysteine hydrolase inhibitor 3-deaza-adenosine prevents oxidative damage and cognitive impairment following folate and vitamin E deprivation in a murine model of age-related, oxidative stress-induced neurodegeneration. *Neuromolecular Med.* 2004; 5:171–180. [PubMed: 15075443]
 22. Smilde T, Berkmortel F, Boers G, Wollersheim H, Boo T, Langen H, Stalenhoef A. Carotid and femoral artery wall thickness and stiffness in patients at risk for cardiovascular disease, with special emphasis on hyperhomocysteinemia. *Arterioscler Thromb Vasc Biol.* 1998; 18:1958–1963. [PubMed: 9848890]
 23. Sood HS, Hunt MJ, Tyagi SC. Peroxisome proliferator ameliorates endothelial dysfunction in a murine model of hyperhomocysteinemia. *Am J Physiol Lung Cell Mol Physiol.* 2003; 284:L333–L341. [PubMed: 12533311]
 24. Sutton-Tyrrell K, Bostom A, Selhub J, Ziegler-Johnson C. High Hcy levels are independently related to isolated systolic hypertension in older adults. *Circulation.* 1997; 96:1745–1749. [PubMed: 9323056]
 25. Tribouilloy CM, Peltier M, Iannetta Peltier MC, Trojette F, Andrejak M, Lesbre JP. Plasma homocysteine and severity of thoracic aortic atherosclerosis. *Chest.* 2000; 118:1685–1689. [PubMed: 11115459]
 26. Tyagi N, Moshal KS, Ovechkin AV, Rodriguez W, Steed M, Henderson B, Roberts AM, Joshua IG, Tyagi SC. Mitochondrial mechanism of oxidative stress and systemic hypertension in hyperhomocysteinemia. *J Cell Biochem.* 2005; 96:665–671. [PubMed: 16149054]
 27. Tyagi SC, Haas SJ, Kumar SG, Reddy HK, Voelker DJ, Hayden MR, Demmy TL, Schmaltz RA, Curtis JJ. Post-transcriptional regulation of extracellular matrix metalloproteinase in human heart end-stage failure secondary to ischemic cardiomyopathy. *J Mol Cell Cardiol.* 1996; 28:1415–1428. [PubMed: 8841929]
 28. Tyagi SC, Matsubara L, Weber KT. Direct extraction and estimation of collagenase(s) activity by zymography in microquantities of rat myocardium and uterus. *Clin Biochem.* 1993; 26:191–198. [PubMed: 8330388]
 29. Watanabe M, Osada J, Aratani Y, Kluckman K, Reddick R, Malinow MR, Maeda N. Mice deficient in cystathionine beta-synthase: animal models for mild and severe homocyst(e)inemia. *Proc Natl Acad Sci USA.* 1995; 92:1585–1589. [PubMed: 7878023]
 30. Whitesall S, Hoff J, Vollmer A, D'Alecy L. Comparison of simultaneous measurement of mouse systolic arterial blood pressure by radiotelemetry and tail-cuff methods. *Am J Physiol Heart Circ Physiol.* 2004; 286:H2408–H2415. [PubMed: 14962829]
 31. Yang F, Tan HM, Wang H. Hyperhomocysteinemia and atherosclerosis. *Sheng Li Xue Bao.* 2005; 57:103–114. [PubMed: 15830093]
 32. Zulli A, Buxton BF, Doolan L, Liu JJ. Augmented effects of methionine and cholesterol in decreasing the elastic lamina while thickening the aortic wall in the rat aorta. *Clin Sci (Lond).* 1998; 95:589–593. [PubMed: 9791045]

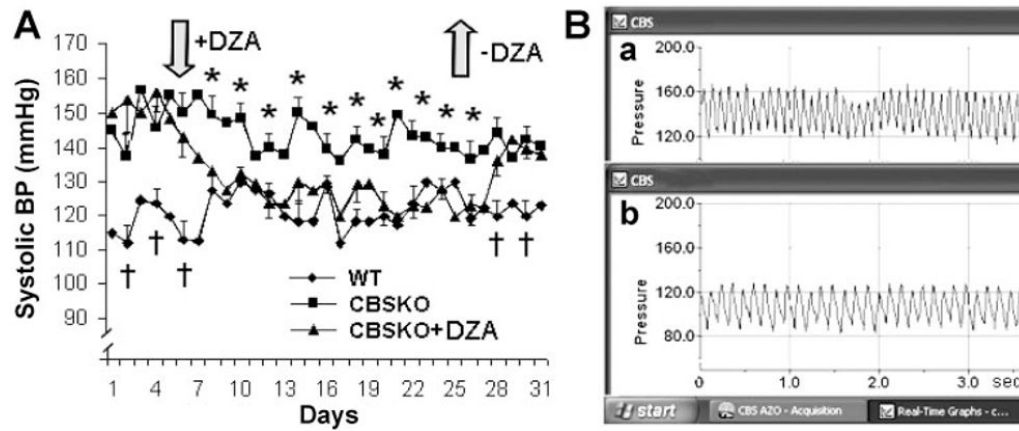


Fig. 1. Aortic blood pressure (BP) in cystathionine α -synthase (CBS) heterozygote ($-/+$) knockout (CBSKO) mice treated with and without 3-deazaadenosine (DZA). *A*: systolic BP during time course of experiment (32 days). Values are means \pm SE; $n = 4$ animals in each group. * \dagger Significant ($P < 0.05$) difference compared with all groups. *B*: telemetric DSI system tracing of systolic (*a*) and diastolic (*b*) BP in real time (3 s). Note that BP and heart rate (based on peak-to-peak intervals), increased in CBSKO mice, were normalized in CBSKO +DZA animals.

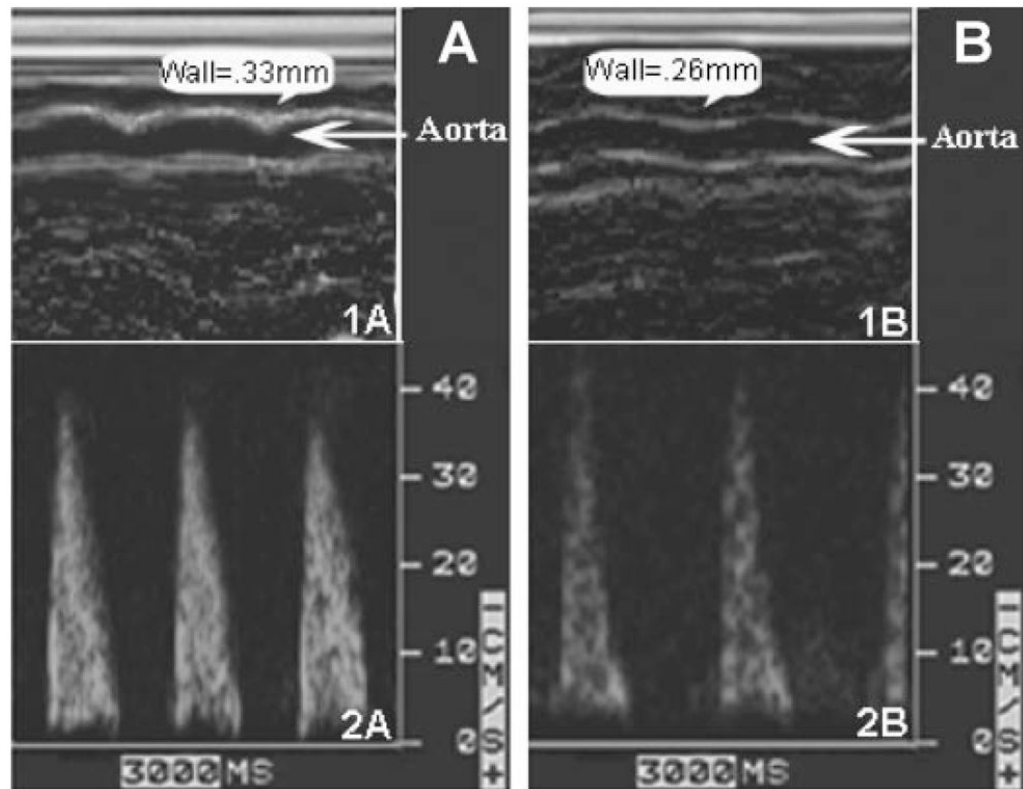


Fig. 2. Thoracic aorta wall thickness (*1A* and *1B*) and time-averaged aortic blood velocity (*2A* and *2B*) in CBSKO mice without treatment (*A*) and with DZA treatment (*B*) obtained by two-dimensionally targeted M-mode and pulsed-wave Doppler echocardiography. Note that aorta wall thickness and blood flow were normalized in CBSKO animals treated with DZA.

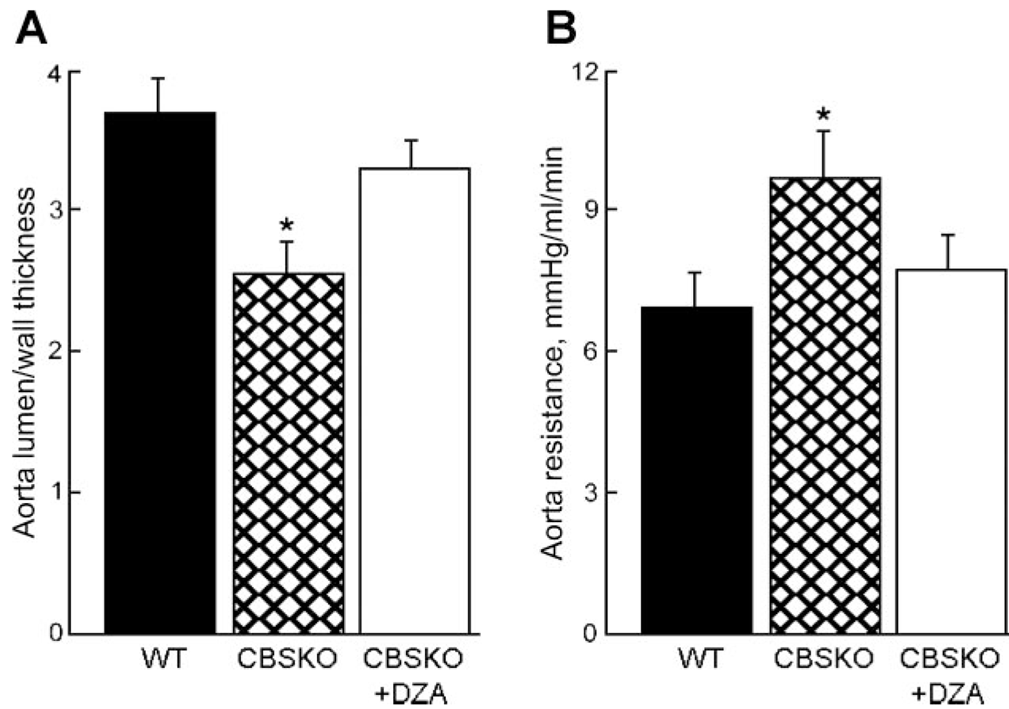


Fig. 3. Thoracic aorta lumen/wall thickness coefficient (A) and aortic resistance (B) in CBSKO mice compared with wild-type (WT) and CBSKO+DZA mice. Values are means \pm SE; $n = 4$ animals in each group. * $P < 0.05$ compared with WT or CBSKO+DZA group.

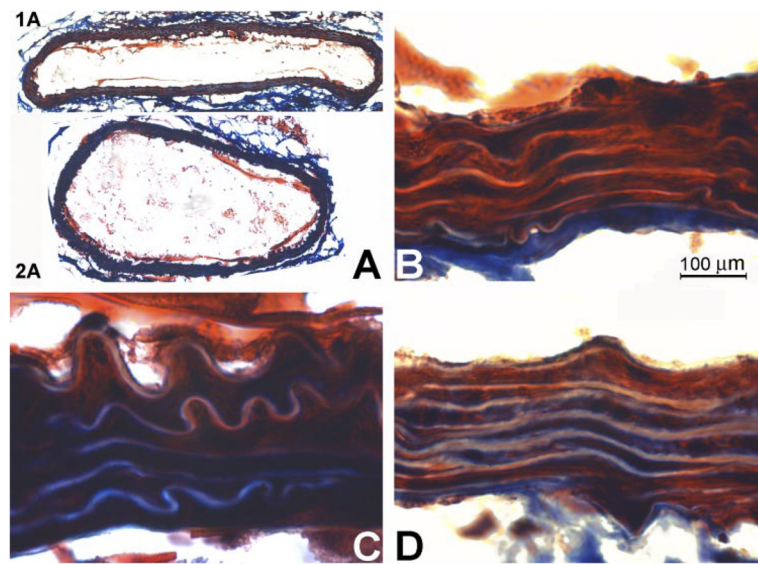


Fig. 4. Histological analysis of aortas in mice treated with and without DZA. Frozen tissue sections were labeled with Masson trichrome staining for collagen (blue). *A*: WT (*1A*) and CBSKO (*2A*) aortic rings ($\times 10$ magnification). *B*: aortic wall from WT mouse. *C*: aortic wall from CBSKO mouse. *D*: aortic wall from CBSKO+DZA mouse ($\times 100$ magnification). Blue color indicates deposition of collagen. Note that the aorta in the CBSKO mouse is hypertrophic and has greater collagen expression than in WT and CBSKO+DZA mice.

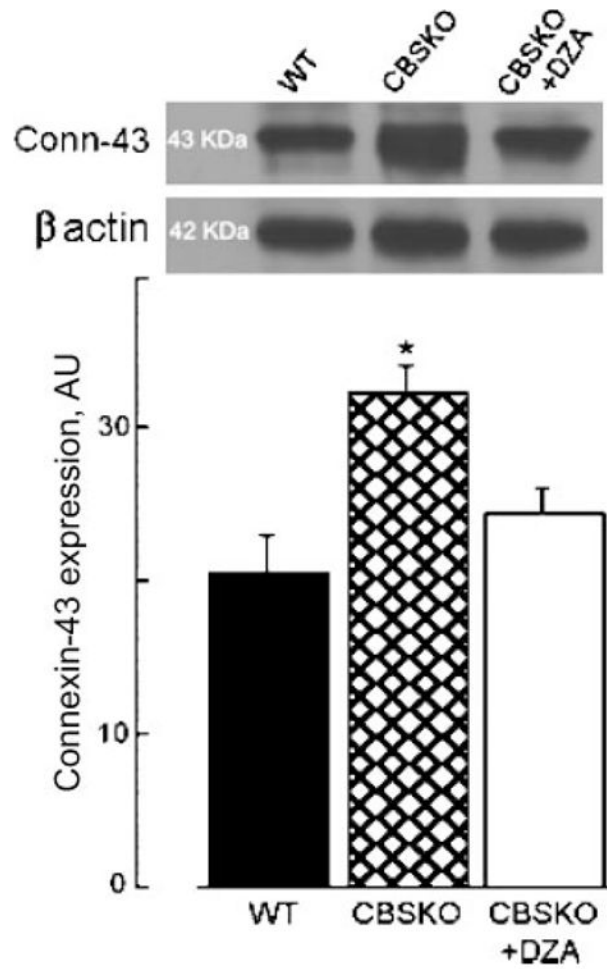


Fig. 5. Connexin 43 expression in aorta from WT, CBSKO, and CBSKO+DZA groups. Values are means \pm SE; $n = 4$ animals in each group. $*P < 0.05$. Note that increase in connexin 43 expression in CBSKO group was prevented in CBSKO+DZA group.

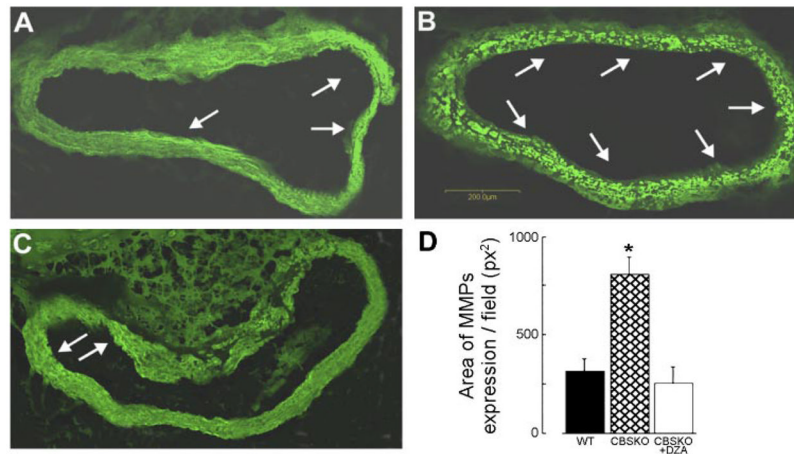


Fig. 6. In situ zymography of matrix metalloproteinase (MMP) activity using DQ gelatin fluorescein-conjugated substrate for MMP in aortic sections from WT (A) and CBSKO mice without (B) or with (C) DZA treatment. Arrows indicate gelatinolytic activity (bright green). D: quantitative analysis of MMP activity. Values are means \pm SE; $n = 4$. *Significant ($P < 0.05$) difference compared with WT or CBSKO+DZA group.

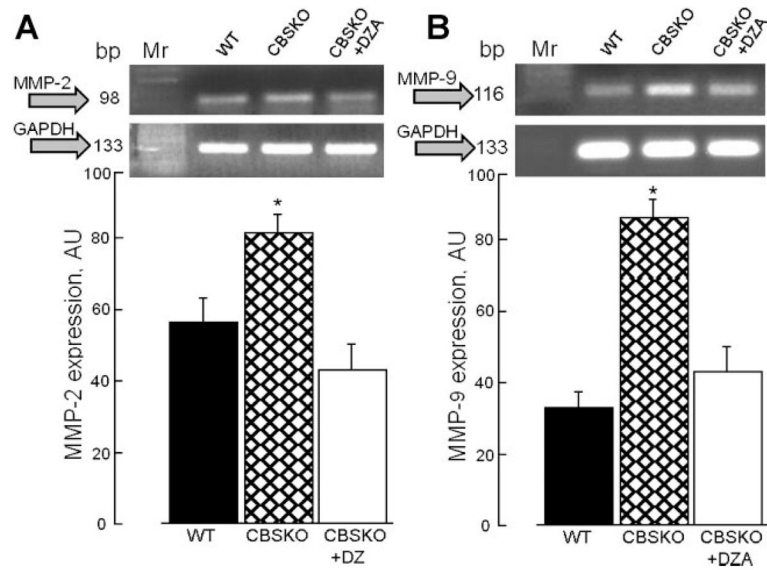


Fig. 7.

Effects of hyperhomocysteinemia on MMP-2 (A) and MMP-9 (B) gene expression in the aorta. Graphs (bottom) represent MMP over glyceraldehyde-3-phosphate dehydrogenase (GAPDH) expression. Values are means \pm SE; $n = 4$ animals in each group; $*P < 0.05$ compared with WT or CBSKO+DZA group. Note that increase in MMP-2 or MMP-9 expression in CBSKO mice was prevented by DZA treatment. AU, arbitrary units.

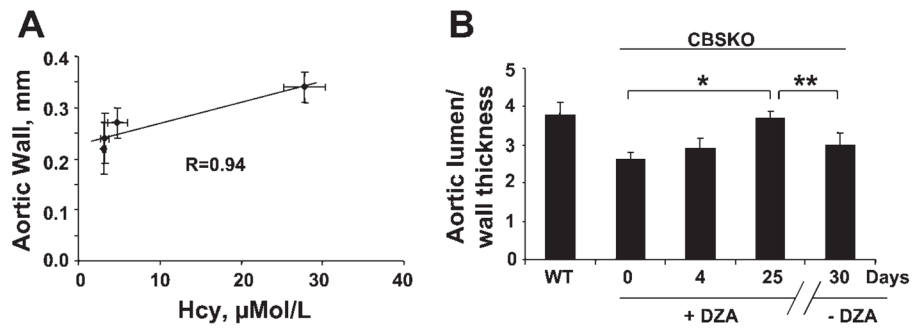


Fig. 8.

A: Correlation between thoracic aorta wall thickness and plasma homocysteine (Hcy) levels: There was a linear relationship (correlation coefficient $R = 0.94$) between wall thickness and plasma Hcy levels. **B:** temporal changes in aortic lumen/wall thickness in WT and CBSKO mice treated with DZA at 0, 4, and 25 days and after removal of DZA at 30 days. $*, **P < 0.05$, 1-way analysis of variance. Values are means \pm SE; $n = 4$ animals in each group.

Table 1

Steady-state physiological parameters in WT, WT + DZA, CBSKO, and CBSKO + DZA mice at 25 days

	WT	WT + DZA	CBSKO	CBSKO + DZA
Plasma Hcy, $\mu\text{mol/l}$	3.2 \pm 0.5	3.1 \pm 0.2	27.8 \pm 2.6*	4.8 \pm 1.2
Body wt, g	29 \pm 0.5	30 \pm 1	30 \pm 0.5	28 \pm 0.5
MAP, mmHg	92 \pm 1	91 \pm 1	130 \pm 1*	93 \pm 1
Heart rate, beats/min	435 \pm 30	426 \pm 31	520 \pm 40*	469 \pm 27
Heart wt, g	0.15 \pm 0.02	0.16 \pm 0.01	0.19 \pm 0.02*	0.17 \pm 0.02
Aortic diameter, mm	1.15 \pm 0.07	1.16 \pm 0.08	1.12 \pm 0.06	1.16 \pm 0.07
Aortic wall thickness, mm	0.24 \pm 0.05	0.22 \pm 0.05	0.34 \pm 0.03*	0.27 \pm 0.03
Time-averaged velocity, cm/s	45.3 \pm 3.1	42.2 \pm 2.9	43.1 \pm 5.2	44.3 \pm 3.2
Aortic blood flow, ml/min	5.8 \pm 0.5	5.7 \pm 0.6	8.1 \pm 0.9*	6.2 \pm 0.7

Values are means \pm SE; $n = 4$ animals in each group. WT, wild type; DZA, 3-deazaadenosine; CBSKO, cystathionine β -synthase heterozygote (-/+) knockout; Hcy, homocysteine; MAP, mean arterial pressure; TAV, aortic blood time-averaged velocity).

* $P < 0.05$ compared to WT or CBSKO + DZA. Note that there were no significant differences between the data obtained from WT and CBSKO + DZA groups.